

## Effect of zirconia addition on the properties of dolomite magnesia refractories used in steel industries

F. Assa <sup>1</sup>, L. Sharifi <sup>\*2</sup>, S.H. Mirhosseini <sup>3</sup>, H. Ajamein <sup>4</sup>, A. Etemad <sup>5</sup>

<sup>1,2,3,4</sup> Modern Ceramic Materials Institute, ACECR, Yazd, Iran

<sup>5</sup> Department of Mining and Metallurgical Engineering, Yazd University, Yazd, Iran

### Abstract

In this study, the influence of the zirconia addition on the properties and microstructure of alkali magnesia refractories without chrome band spinels was investigated. For this purpose, a primary formula based on magnesia and alumina to form spinel was considered, and different amounts of zirconia were added to achieve various samples. After thermal treatment at 1500 °C and 1600 °C, the physical and mechanical properties of fabricated samples such as density, apparent porosity, cold compressive and bending strength, refractoriness under load, and warm modulus of rupture according to ASTM were evaluated. The physical and mechanical properties of zirconia contained samples revealed that the addition of zirconia led to the formation of zirconate-based phases like magnesium zirconate, and calcium zirconate. This phase can be expanded by the thermal stresses due to its thermal mismatch with the phases of the field and improved the mechanical properties by creating microcracks in the structure. Addition of 2% by weight of zirconia increased the density from 2.8 g/cm<sup>3</sup> to 2.95 g/cm<sup>3</sup> at 1600 °C. Compressive strength also increased from 315 kg/cm<sup>2</sup> to 550 kg/cm<sup>2</sup> and flexural strength from 35 kg/cm<sup>2</sup> to 65 kg/cm<sup>2</sup>.

*Keywords:* Refractories material, Magnesia alkaline brick, Zirconia, Spinel phase.

### 1. Introduction

Alkaline bricks, especially magnesia refractory products containing spinel, are the most important refractory materials. Due to their special physical, chemical and mechanical properties, they are used in many refractory industries such as steel,

cement, and non-ferrous industries <sup>1-4</sup>). The steel industry is one of the main industries consuming refracting materials. Alkaline bricks are generally used in furnaces to prevent chemical corrosion <sup>5, 6</sup>).

Today, the use of magnesium alkali refractory bricks is very popular in steel industry furnaces due to its remarkable physical and mechanical properties as well as high refractoriness, and corrosion resistance against alkaline corrosive agents <sup>7-9</sup>). However, due to its high thermal expansion coefficient and low thermal shock resistance, some problems such as physical and thermomechanical properties as well as thermal shock resistance occur in the application of this type of refractories in the steel industry. Applying additives in small amount is one of the ways to solve these problems, which can reduce the above defects to increase the shockability of these refractories <sup>10, 11</sup>).

*\*Corresponding author*

*Email: sharifi.leila.jd@gmail.com*

*Address: Modern Ceramic Materials Institute, ACECR, Yazd, Iran*

*1.M.Sc*

*2.Assistant Professor*

*3.Assistant Professor*

*4 Assistant Professor*

*5.Ph.D. Student*

Chromium-containing compounds were among the first additives used in the manufacture of magnesia bricks. However, the use of these materials improved the properties of magnesium refractories, but excessive toxicity as well as adverse and destructive effects on the environment due to the presence of hexavalent chromium ions in magnesia-chromite brick waste of rotary kilns eventually led to the development of chromium-free magnesia alkaline bricks<sup>11-13</sup>. Magnesium aluminate spinel were one of the important additives that was used as the main component in magnesia-spinel bricks and facilitates the use of magnesia-spinel bricks for industrial applications from 1980<sup>14</sup>. Although magnesia-spinel bricks have good hot properties, excellent shockability, and good resistance to regenerative atmospheres, they have several weaknesses in terms of properties such as resistance to melt penetration as well as coatability<sup>15-17</sup>. It is now known that additives such as  $\text{Fe}_2\text{O}_3$ ,  $\text{ZrO}_2$ , and  $\text{TiO}_2$  increase the coatability of these products. Despite the high cost of producing, these refractories are cost effective due to their long service life in steel furnaces<sup>18, 19</sup>. In this research,  $\text{ZrO}_2$  additive has been used for magnesia-spinel refractories to eliminate defects and improve various properties, including physical properties (appearance porosity, density), thermomechanical (refractory under load and hot flexural strength), mechanical (cold flexural strength and cold compressive strength), corrosion resistance and coatability. Furthermore, the formation of different

phases in the presence of additives and the role of each on the properties and behavior of sintering were studied by analyzing the cold and hot mechanical properties, how to create spinel phases and their role on changing properties.

## 2. Materials and methods

### 2.1. Raw materials

Magnesia is the most important refractory raw material of the samples studied in this research. Since magnesia is a major component of body formulations, in the design of refractory samples, the quality of magnesium used will have a very important effect on all properties and characteristics after sintering such as purity, ratio, density and porosity, bonding phases and granulation distribution. In this study, Iranian zinc magnesia with a purity of more than 96% has been used. Table 1 shows the chemical analysis of consumed magnesia performed by wet chemistry method.

Spinel is the second component of the fabricated refractory. Depending on the amount of alumina or excess magnesia, this material will have a direct impact on the sintering behavior of the samples. The spinel used in this research is a type of magnesia-rich sinter spinel produced by Alcoa USA with the code AR78 and purity of more than 99% and a particle size range of 0-0.5mm. The chemical analysis of this substance, which was performed by the wet chemistry method, is given in Table 2.

Table 1. Chemical analysis and density of magnesia primary material.

Oxide	Purity (wt%)
MgO	96.22
CaO	1.62
$\text{Al}_2\text{O}_3$	0.25
$\text{Fe}_2\text{O}_3$	0.82
$\text{SiO}_2$	0.6
L.O.I	0.28
B.D ( $\text{g}/\text{cm}^3$ )	3.25

Table 2. Chemical analysis of consumed spinel.

Oxide	Purity (wt%)
MgO	33.00
CaO	<0.01
$\text{Al}_2\text{O}_3$	64.00
$\text{Fe}_2\text{O}_3$	<0.01
$\text{SiO}_2$	0.50
L.O.I	0.65
B.D ( $\text{g}/\text{cm}^3$ )	3.28

Alumina is another major and relatively pure raw material used in the refractory industry, which has several types. One of the most important types of alumina is plate-shaped alumina (alumina tabular), which is a type of high purity aluminum oxide and in its production, through temperature control, alpha-alumina crystals are converted into large crystalline grains (corundum phase). Alumina is the third component of fabricated refractory sample, which is a type of alumina tabular product of Almatix Company in France with code T60 / T40, with a purity of 99.5% and a particle size range of 0-0.5mm. Table 3 shows the chemical analysis of consumable alumina tubular.

Table 3. Chemical analysis of consumable tabular alumina.

Oxide	Purity (wt%)
Al <sub>2</sub> O <sub>3</sub>	99.5
CaO+MgO	< 0.4
Na <sub>2</sub> O+K <sub>2</sub> O	<0.5
B.D (g/cm <sup>3</sup> )	3.55

Applied zirconia additive is stabilized with 3% yttrium and 99.5% chemical purity from Tosoh Company in Japan. The average particle size of this product is in the range of 0.5 microns. Due to the ability to perform phase transformation and change in volume due to temperature, this material has the ability to form micro-cracks in the field of ceramic composites, which can improve the strength and failure of ceramics and refractory materials. Table 4 shows the chemical analysis of consumed zirconia.

Table 4. XRF chemical analysis of consumed zirconia.

Oxide	Purity (wt%)
HfO <sub>2</sub>	5.02
Na <sub>2</sub> O	< 0.01
Al <sub>2</sub> O <sub>3</sub>	<0.01
Fe <sub>2</sub> O <sub>3</sub>	<0.01
ZrO <sub>2</sub>	99.50
Y <sub>2</sub> O <sub>3</sub>	5.22
B.D (g/cm <sup>3</sup> )	6.05

## 2.2. Preparation of samples

In order to prepare the samples, for each formulation, large and medium particles were first mixed together for 5-7 minutes. At this stage, 3% of the MgCl<sub>2</sub> binder was added and mixed for another 5 minutes. Then, the powder component was added and the mixing operation continued for another 5-7 minutes. The total mixing time for each formula was 15 to 20 minutes and the amount of samples was equal to 20 kg. Mixing was done manually

in plastic containers. Also, additives were mixed with fine-grained components of refractory formulation due to their better dispersion in the field of refractory materials. The samples were formed as bricks by the hydraulic press with a pressure of 1200 kg / cm<sup>3</sup>. Also, for more detailed studies, a number of samples were pressed into small cylinders. The dimensions of the mold intended for making brick samples were 198 × 200 mm.

After pressing and shaping, the samples were dried for 24 hours at 110 °C. The drying step is very important and sensitive due to the role of moisture was added during the forming step. If the moisture of sample was not removed carefully and cautiously at this stage, samples are likely to crack, especially for larger samples, in the early stages of sintering and when the temperature rises sharply.

In the sintering stage, the correct choice of temperature and duration of heat treatment along with the correct design of the heat regime and the selection of the optimal heating rate have a strong effect on creating defectless samples. In order to achieve bodies with suitable density, two different maximum sintering temperatures were selected. For this purpose, the samples were sintered at 1500 °C and 1600°C in a shuttle oven. The samples were heated at maximum temperature for 6 hours and the whole sintering process took about 55 hours.

## 3.2. Determining the properties of samples

In this study, the density and apparent porosity of the samples were measured by immersion test according to the ASTM-C830 standard. To perform these experiments, in order to ensure the accuracy of the results, measurements were made from 5 samples and the average results were reported. Another important parameter in comparing the properties of refractory materials and products is the measurement of strength properties (according to ASTM-C133). In this experiment, measurements were taken from at least 3 samples and the average results were reported. The cold compressive strength measuring device is made by EKO Company in Japan and the model of the device is TSA-522.

Cold flexural strength is the resistance of refractory bricks to the bending forces applied to them, which is another important test in the study of the mechanical properties of refractory materials. In this research, ASTM-C583 standard has been used to evaluate this feature. In this experiment, measurements were taken from at least 3 samples and the average results were reported. The cold bending strength measuring device is made by EKO Company in Japan and the model is JAN-1992. In the hot flexural strength test, the specimen must be heated in a special furnace with a specified heat gradient to a certain temperature at the moment of load application. The higher the flexural strength of the part at high temperature, the better its performance at room temperature or the desired application temperature. ASTM-C64 standard was used to measure this parameter.

In this experiment, measurements were taken from at least 3 samples and the average results were reported. The hot flexural strength measuring device is made by EKO Company of Japan and the model is TSA-522.

Another feature that shows the thermomechanical behavior of refractories in real application conditions is the degree of refractory under load. This test was performed according to the ASTM-C113 standard. In this experiment, measurements were taken from at least 2 samples and the average results were reported. The model of RUL device used was TSAR-612 and made in Japan. Samples were studied by scanning electron microscopy (SEM) to study the developments and the type of connection between the grains and the ground phase after the sintering process and the type of phases formed in the grain boundaries in order to better understand the sintering mechanisms. To examine the microstructure of the samples, a scanning electron microscope made by TESCAN VEGA of the Czech Republic was used. In order to study the phase changes of the samples after baking, an X-ray diffractometer made by PHILIPS model 3710 PW was used. In order to study the chemical analysis of some of the raw materials used in this research, the method of chemical analysis by X-ray fluorescence (XRF) with an XRF device made by PHILIPS Company was used.

### 3. Results and Discussion

#### 3.1. Stable linear changes

Figure 1 shows the stable linear changes of samples

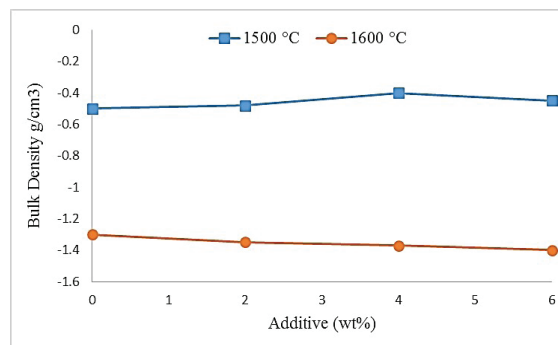


Fig. 1. Stable linear changes of samples containing zirconia additive after curing at 1500 °C and 1600 °C.

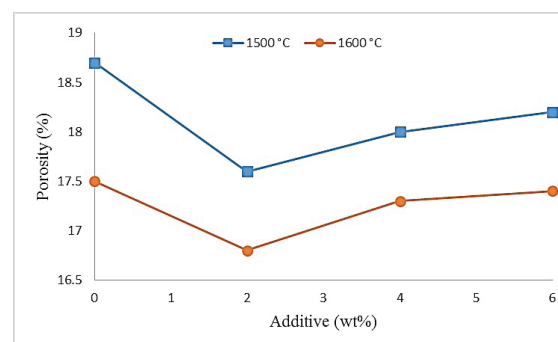


Fig. 2. Porosity of samples containing zirconia after curing at 1500 °C and 1600 °C.

containing zirconia additive. With an increasing percentage of zirconia in samples sintered at 1500 °C, a slight increase and then a decrease compared to the reference sample without additive is observed. The increase in relative dimensions can be due to the increase in the amount of spinel phase as well as the formation of zirconate phases. Also, with increasing temperature to 1600°C, linearly reduce dimensions are observed compared to the reference sample without additives. It seems that with the formation of more zirconate phases at this temperature and the reaction of zirconia with magnesium and alumina in the sample structure has contracted.

#### 3.2. Density and porosity

Figures 2 and 3 show the trend of density changes and apparent porosity of zirconia-containing samples by increasing the percentage of the additive at different sintering temperatures, respectively. As can be seen in these figures, for samples containing zirconia, there is a clear difference between the density and porosity of the samples containing the additive and the reference sample, which indicates the effect of increasing the amount of these additives in the sintering process. According to these graphs, with increasing zirconia up to 6% compared to the sample with out additives, the density increases and the apparent porosity decreases.

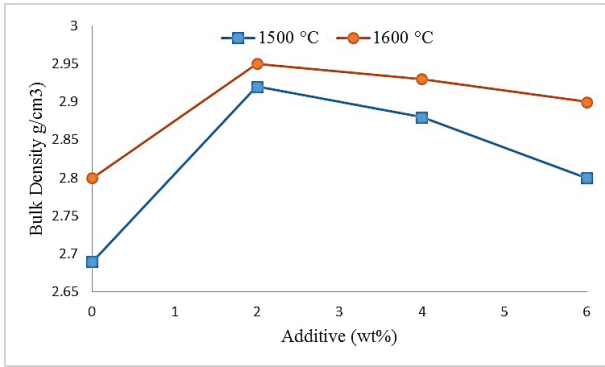


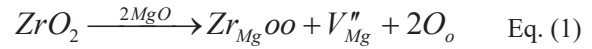
Fig. 3. Bulk Density of samples containing zirconia after curing at 1500 °C and 1600 ° C.

In the system containing zirconia additive, the formation of phases such as magnesium zirconate ( $M_2Z$ ,  $MZ_2$ ,  $MZ$ ), aluminate-magnesium spinel and iron-calcium zirconate and calcium zirconate due to the reaction of zirconia and magnesia in the composition causes expansion. Therefore, it is expected that with increasing the amount of fine-grained zirconia additive in the field of refractory and the formation of the above phases compared to the sample without additives, porosity decreases and density increases. On the other hand, phases such as magnesium zirconate formed due to the reaction of zirconia particles with magnesia in the field are able to increase the strength by creating a strong bond in the refractory field between the magnesia and spinel particles as well as the magnesium field. This is while the pre-synthesized spinel phase in the system, due to the mismatch of the thermal behavior with the magnesia around it, creates cracks that prevent a strong connection. As a result, the amount and type of structure of magnesium zirconate phases play a key role in the amount of porosity and strength of magnesia-spinel refractories. In this case, the important factors of reducing porosity based on the formation of magnesium zirconate phases and the formation of micro-cracks due to non-compliance of the thermal behavior of spinel and magnesia are effective in this regard.

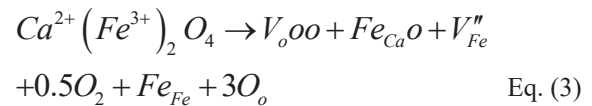
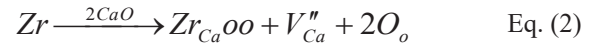
On the other hand, the density of refractory samples naturally depends on the density of each component of the system. Therefore, it is expected that with increasing the amount of zirconia oxide fine-grained additives in the refractory field, the porosity decreases and the density increases compared to the reference sample without additives. However, the reason for the increase in porosity and decrease in density with increasing the amount of oxide additives from 2 to 6% depends on the volume percentage of the expansion phases. In other words, increasing the phases associated with volumetric expansion has reduced the density and increased the porosity compared to samples with 2% additive.

On the other hand, according to reaction 1, with the dissolution of zirconia oxide additive in the periclass

network, due to the difference in ion capacity of  $Zr^{4+}$  with  $Mg^{2+}$  by replacing an ion  $Zr^{4+}$  Instead of  $Mg^{2+}$  an ion  $Mg^{2+}$  should be removed causing pitting cations network. The formation of these cavities increases the diffusion coefficient and ultimately encourages the mass transfer and sintering process. Therefore, it is expected that as the amount of zirconia oxide additives increases, the body density increases and the porosity decreases.



In addition, the dissolution of oxides such as  $ZrO_2$  in the spinel network and the removal of Al from the network in the stoichiometric composition can also improve sintering. In fact, the dissolution of zirconia in the magnesia and alumina phases and the creation of atomic voids encourage the formation of a spinel phase. In this case, in the presence of other impurities such as  $Fe_2O_3$  and  $CaO$  due to the formation of the liquid phase, the presence of these phases, in addition to encouraging the sintering process, can be used as a germination agent that causes crystallization of iron-calcium zirconate phases simultaneous formation of magnesium zirconate and magnesium aluminate spinel phases occurs from the melt, a phenomenon that has been demonstrated during reactions 2 and 3.



### 3.3. Mechanical properties

Figures 4 and 5 show cold compressive and flexural strength diagrams of zirconia-containing specimens after sintering at different temperatures, respectively. At both backing temperatures, the amount of cold compressive strength and flexural strength increases with an increasing amount of zirconia additive compared to the reference sample without additive. But with increasing the amount of additive to 4 and 6%, the values of these parameters have decreased slightly. This is true for all samples containing zirconia. It seems that the strength and mechanical properties of these specimens are strongly dependent on how they are compacted and compacted. In other words, as the porosity increases, the strength values decrease. Basically, a set of different factors can affect the mechanical strength of samples.

According to study sources, one of these factors is the formation of micro-cracks and especially the degree of porosity, which has led to small amounts of MOR and CCS in the reference refractory sample without additives. However, cracks are formed due to the formation of spinel phases and phases that are

formed due to the mismatch of spinel thermal behavior with magnesia with volumetric expansion. They can be effective in increasing strength and strengthening the mechanical properties of the body. Therefore, it seems that the mechanism of micro crack formation is dominant here, because with increasing the amount of zirconia, the formation of spinel phases has increased, which is further discussed in the microstructure study section.

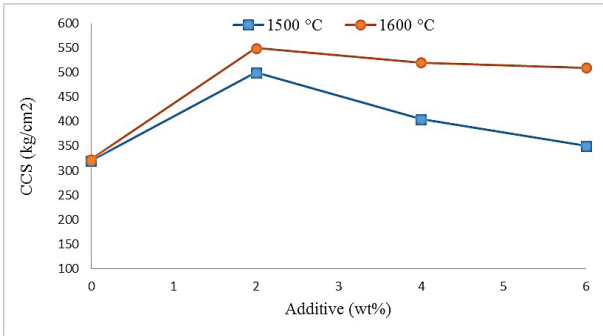


Fig. 4. Compressive strength of zirconia-containing samples after curing at 1500 °C and 1600 °C.

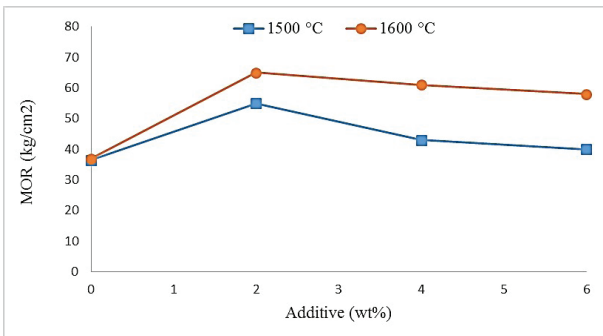


Fig. 5. Modulus of rupture of samples containing zirconia after curing at 1500 °C and 1600 °C.

In general, according to Figures 4 and 5, the strength increases with increasing amount of oxide additives. Various factors increase the strength, such as higher density of the body with increasing amounts

of zirconia and also their interaction with micro-cracks around the spinel particles are among these factors. In addition, this oxide, due to the help of the sinter, causes the critical cracks to deviate due to the difference in the coefficient of thermal expansion of magnesia and spinel, which also increases the strength.

Another reason for the increased strength of zirconia-containing specimens is the dissolution of quaternary zirconium ions and the exit of trivalent Al ions from the spinel lattice, which causes the spinel structure to expand. As a result of this phenomenon, the field density increases and the porosity decreases as much as possible, and finally, the cold strength of the samples will increase.

It should be noted, however, that the presence of zirconium ions in the composition also delays the dissolution of Al<sup>3+</sup> ions within the spinel network. Because the dissolution of Zr<sup>4+</sup> according to Hume-Rotary theory occurs faster inside the spinel lattice than Al<sup>3+</sup> ions, which will result in more expansion in the field with a constant increase of lattice. Therefore, it should be said that what affects the properties of the desired bodies, especially the mechanical properties, is a set of factors mentioned above.

### 3.4. Thermomechanical properties

Figure 6 shows a diagram of changes in hot flexural strength (HMOR) of a sample containing zirconia additive. As can be seen, with the addition of zirconia up to 6% of the hot flexural strength of the specimens compared to the reference specimen without addition at 1000°C and 1400 °C has been increased. It can be said that this is due to the strong bonds that these oxides have created in the field. The formation of phases such as spinel phases of zirconate-magnesium and aluminate-magnesium can also be effective in this regard. Another reason for the increase in hot flexural strength by increasing the oxide additives by up to 6% is the dissolution of Zr<sup>4+</sup> in the periclas lattice of direct reaction of magnesia with tubular alumina. In other words, in this case, the simultaneous formation of magnesium zirconate and magnesium aluminate spinel phases occurs.

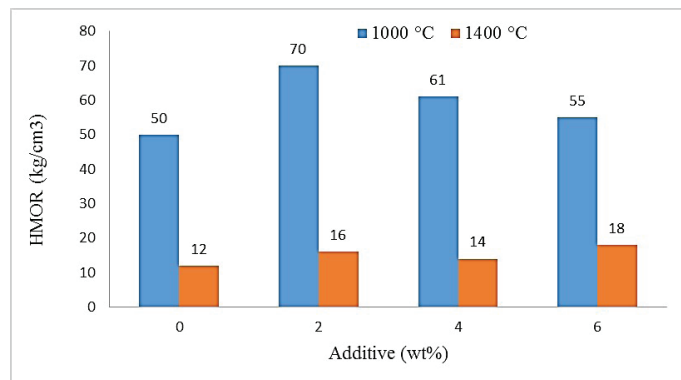
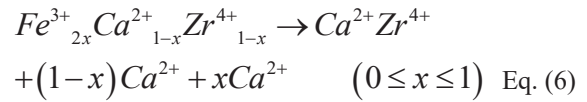
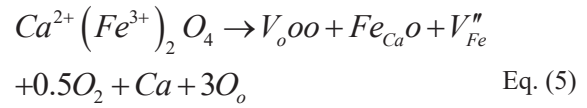


Fig. 6. Hot modulus of rupture of zirconia-containing specimens at 1000 °C and 1400 °C.

According to this diagram, it can be seen that the hot flexural strength of the sample has decreased at 1400 ° C compared to 1000 ° C. This is due to the growth of microcracks and the formation of possible pre-melting phases in the grain boundary regions such as zirconate-calcium, zirconate-iron and calcium-iron phases due to the reaction of zirconia with iron and calcium oxide in magnesia raw material. By increasing the amount of zirconia to 6%, the pre-melting phases in the grain boundary areas are reduced, which increases the hot flexural strength of samples containing 6% additive at 1400°C.

According to the reactions of 4 and 5 phases, iron-calcium zirconate reduced the hot flexural strength of the samples at 1400 °C. Because at high temperatures it is possible to decompose this phase into two phases of iron zirconate and calcium zirconate or iron-calcium phase, Therefore, on the one hand, the warm strength is expected to decrease, and on the other hand, the grain morphology is likely to change at high temperatures due to the reaction of magnesia with zirconia, which affects the strength of the sintered products.



### 3.5. Phase analysis

Figures 7 and 8 show the X-ray diffraction patterns of the reference sample (without additives) cooked at 1500 and 1600 ° C, respectively.

As can be seen, the Phase analysis of this sample at a lower sintering temperature includes periclase (MgO) and spinel (MgAl<sub>2</sub>O<sub>4</sub>) phases. It is also observed that there is no trace of residual phases containing alumina and it can be concluded that the reaction of alumina with magnesia and the formation of spinel phase at 1500 °C has been completed. However, given the peak intensity of the phases shown in Figures 7 and 8, it appears that the spinel grain size has grown more relative at 1600°C.

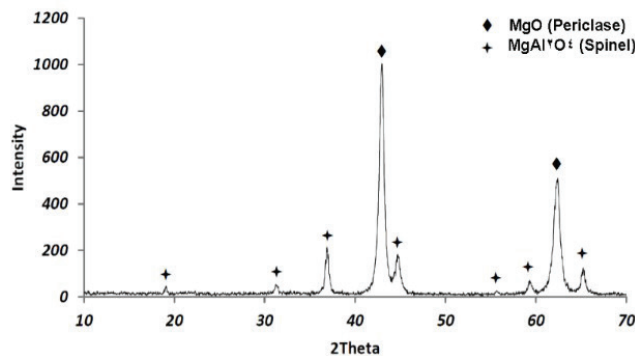


Fig. 7. X-ray diffraction pattern of the reference sample cooked at 1500 °C.

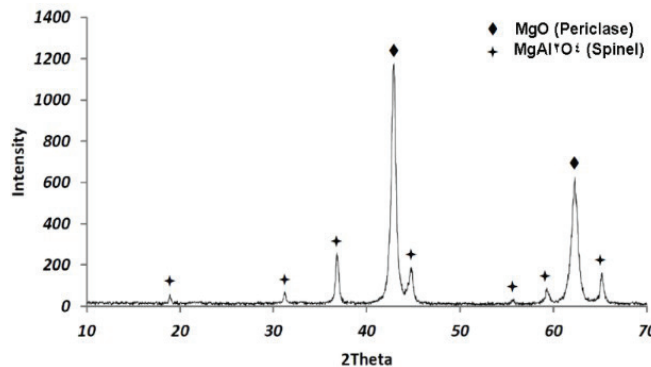


Fig. 8. X-ray diffraction pattern of reference sample cooked at 1600 °C.

Figures 9 and 10 show X-ray diffraction patterns of samples containing 4% zirconia additive after firing at 1500 and 1600 ° C, respectively. Figure 9 shows the sample cooked at 1500 ° C with the main phases of periclase and spinel. Figure 9 shows the sample cooked at 1500 ° C with the main phases of periclase and spinel. However, the presence of new phases of a new solid solution based (Mg, Al, Zr, O) with lower intensities can also be observed in this sample. Also, here is a small amount of spinel phase deviation to the right, which indicates the creation of empty spaces in the spinel network and the contraction of its network relative to the reference sample without additives. Also, according to Figure 10, it can be seen that at 1600 ° C, the formation of these phases has been done with more temperature increase.

### 3.6. Microstructure

In this section, the microstructure and context of samples containing various additives made in this research by electron microscopy (SEM.EDS) are discussed. First, the reference sample microstructures are given and then the sample microstructures containing zirconia are given.

Figure 11 shows the microstructure of the reference sample (no additive) sintered at 1600 ° C.

Figure 12 also shows the microstructure and elemental analysis (point) of the four specified points of the reference sample microstructure. As can be seen, in grain boundaries (grain boundary of magnesia-magnesia and magnesia-spinel particles), the calcium silicate phase is formed along with magnesiofrite phase (gray dots) which has a direct effect on the density and porosity of bodies.

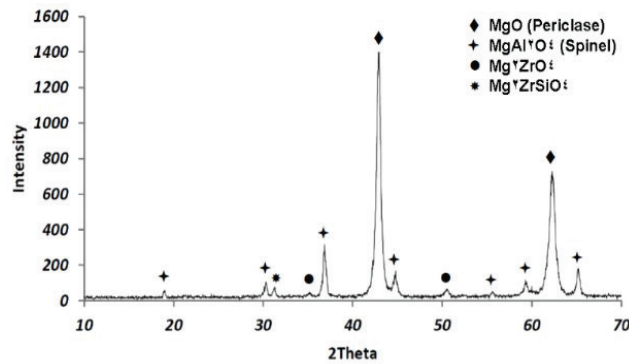


Fig. 9. X-ray diffraction pattern of a sample containing 4% zirconia cooked at 1500 ° C.

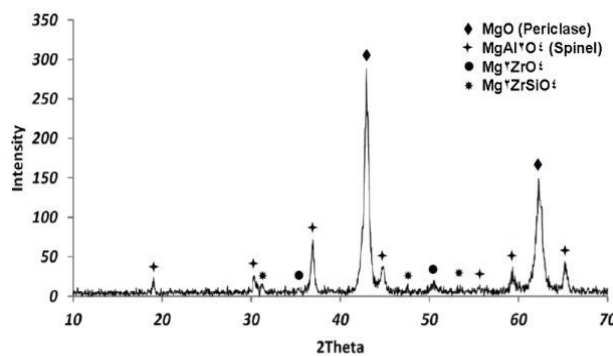


Fig. 10. X-ray diffraction pattern of a sample containing 4% zirconia cooked at 1600 ° C.

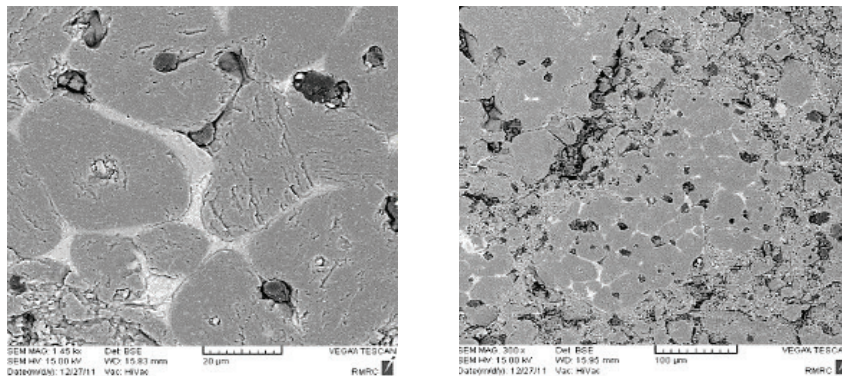


Fig. 11. Microstructure of the sintered reference sample at 1600 ° C.



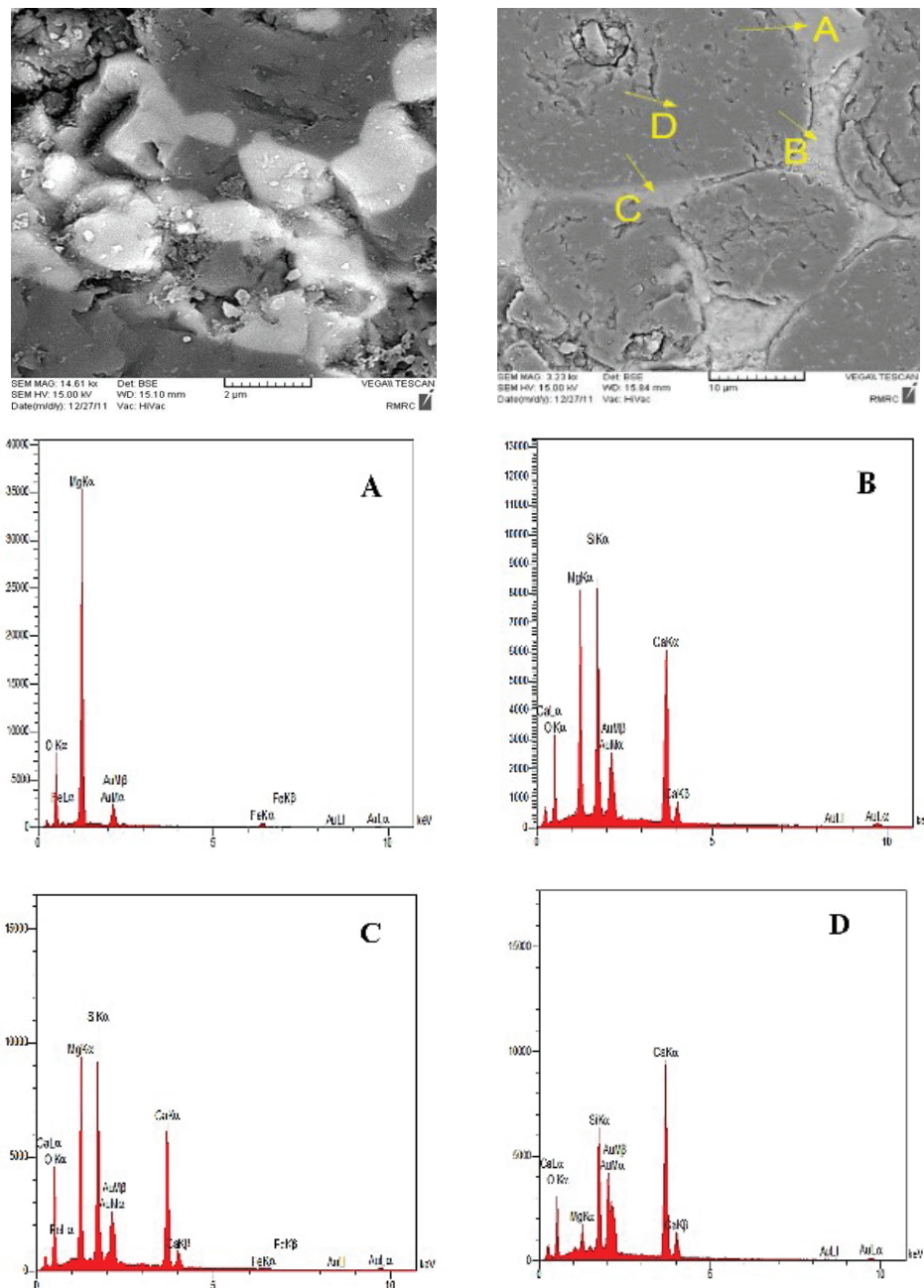


Fig. 12. Microstructure and elemental analysis of the four specified points of the sintered reference sample at 1600 °C.

As explained in the discussion of the results of the physical properties, given that the magnesium used in this study has a relatively high purity, Therefore, another effective factor in reducing porosity and increasing density can be the second mechanism, i.e. increasing vacancy and penetration coefficient.

Figures 13 and 14 show the microstructure and elemental analysis of the sample containing 6% sintered zirconia at 1600 °C. These images show the formation of the phases of magnesium zirconate, magnesium aluminate spinel, and iron-calcium zirconate at the Magnesia-Magnesia and Magnesia-Spinel grain boundaries, as well as within the magnesia grains resulting from the direct

reaction. As shown in Figure 13,  $ZrO_2$  reacts with the CaO in magnesia to form the perovskite phase of calcium zirconate at the grain boundary, which in turn leads to a stronger bond between the magnesia and spinel grains. On the other hand, due to the fineness of the zirconia particles used, the diffusion intervals are reduced and as a result, the zirconate-calcium phase is formed more easily.

These images show that zirconia additive can also play an effective role in increasing the density of the refractory body by increasing the cationic void. Reaction 6 shows the formation mechanism of the solid solution phase of magnesium zirconate.



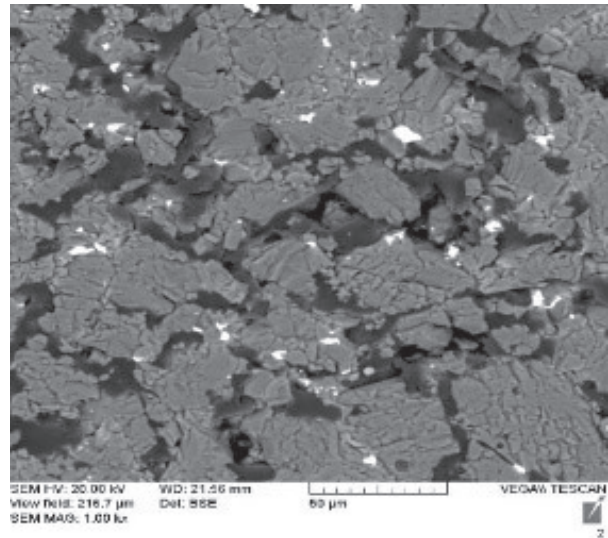
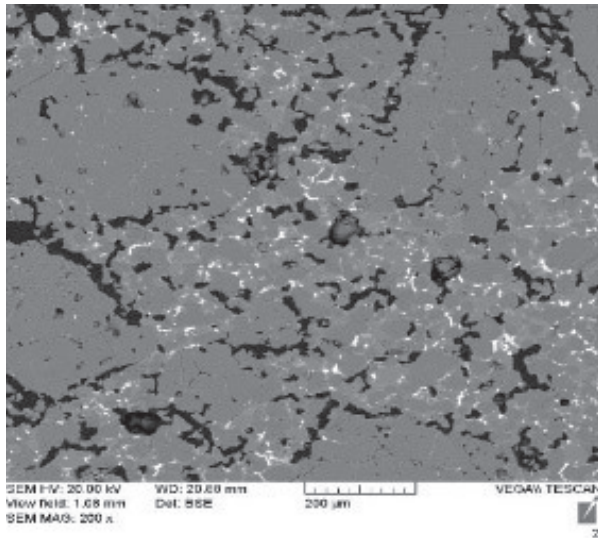


Fig. 13. Sample microstructure containing 6% sintered zirconia at 1600 °C.

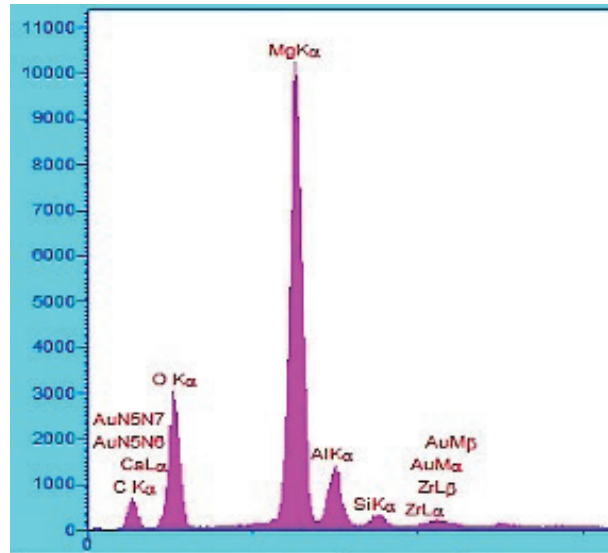
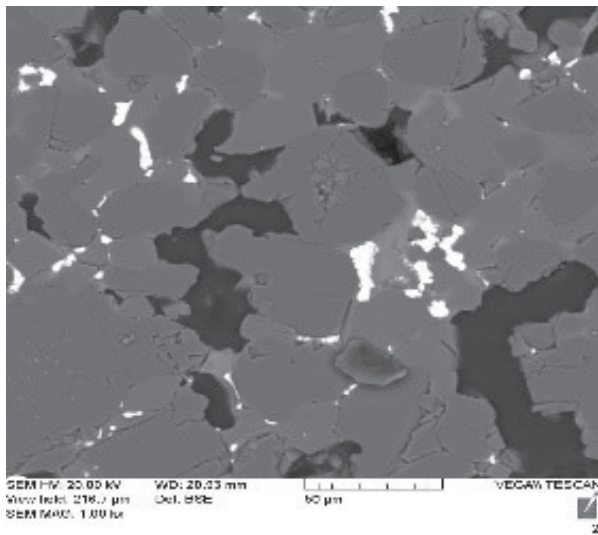


Fig. 14. Microstructure and elemental analysis of zirconate phase in a sample containing 6% zirconia sintered at 1600 °C.

#### 4. Conclusions

- This study was performed on different physical, mechanical, thermomechanical, phase and microstructural properties of samples containing different percentages of zirconia additive in Magnesia-Spinel refractory system.
- Although the proposed system with relatively no additives (reference system) shows relatively good physical and mechanical properties, However, the addition of some additives such as zirconia improves and intensifies some properties, especially physical, mechanical and thermomechanical properties.
- Also the phases of iron zirconate and magnesium zirconate in bricks with the phase of calcium zirconate which is caused by the reaction of zirconia in the

brick with CaO in the melt, reacts and improves brick coverage.

- In this case, the addition of zirconia causes the formation of a protective layer at the joint of brick and melt and leads to the formation of a coating on this layer and increases its lifespan.
- According to the phase and microstructural analyzes, it was observed that the addition of zirconia to the studied system leads to the production of zirconate-based phases such as magnesium or calcium zirconate. Due to the thermal incompatibility with the ground phases, this phase can expand the field due to thermal stresses and improve the mechanical properties by creating microcracks in the system.

## Reference

- [1] C. Sadik, O. Moudden, A. El Bouari, I.-E. El Amrani: *J. Asian Ceram. Soc.*, 4(2016), 219.
- [2] S.Ghasemi-Kahrizsangi, H.G. Dehsheikh, E. Karamian, M. Boroujerdnia, K. Payandeh: *Ceram. Int.*, 43(2017), 5014.
- [3] S.Ghasemi-Kahrizsangi, E. Karamian, H.G. Dehsheikh: *Ceram. Int.*, 43(2017), 13932.
- [4] S.Ghasemi-Kahrizsangi, E. Karamian, H. Gheisari Dehsheikh, A. Ghasemi-Kahrizsangi: *J. Water Environ. Nanotechnol.*, 2(2017), 206.
- [5] S.Ghasemi-Kahrizsangi, H. Gheisari-dehsheikh, M. Boroujerdnia: *Iran. J. Mater. Sci.*, 13(2016), 33.
- [6] R. Kusiorowski, J. Wojsa, B. Psiuk, T. Wala: *Ceram. Int.*, 42(2016), 11373.
- [7] L. Horckmans, P. Nielsen, P. Dierckx, A. Ducastel: *Resour. Conserv. Recycl.*, 140(2019), 297.
- [8] M. Beyhaghi, M. Rouhani, J. Hobley, Y.-R. Jeng: *Appl. Surf. Sci.*, 569(2021), 151037.
- [9] M. Beyhaghi, A.-R. Kiani-Rashid, M. Kashefi, J.V. Khaki, S. Jonsson: *Appl. Surf. Sci.*, 344(2015), 1.
- [10] M. Krishnan, R. Manikandan, D. Thenmuhil: *Ceram. Int.*, 47(2021), 3430.
- [11] M. Mohammadihooyeh, E. Karamian, R. Emadi: *Ceram. Int.*, 46(2020), 1662.
- [12] S. Ghasemi-Kahrizsangi, H.G. Dehsheikh, E. Karamian, A. Nemati: *Ceram. Int.*, 44(2018), 2058.
- [13] C. Gómez-Rodríguez, D. Fernández-González, L.V. García-Quiñonez, G.A. Castillo-Rodríguez, J.A. Aguilar-Martínez, L.F. Verdeja: *Metals*, 9(2019), 1297.
- [14] S. Otraj, A. Daghighi: *Ceram. Int.*, 37(2011), 1003.
- [15] A. Kumar, P. Kumar, A. Ghosh, S. Sinhamahapatra, H.S. Tripathi: *Int. J. Miner. Process.*, 144(2015), 40.
- [16] R. Kusiorowski: *Constr. Build. Mater.*, 231(2020), 117084.
- [17] M. Beyhaghi, M. Kashefi, A. Kiani-Rashid, J. Vahdati Khaki, S. Jonsson: *Surf. Coat. Tech.*, 272(2015), 254.
- [18] S. G. Kahrizsangi, A. Nemati, A. Shahraki, M. Farooghi: *Int. J. Nanosci. Nanotechnol.*, 12(2016), 19.
- [19] M. Mohammadihooyeh, E. Karamian, R. Emadi: *Ceram. Int.*, 45(2019), 20674.